Atmospheric Water Harvesting by Large-Scale Radiative Cooling Cellulose-Based Fabric

Yun Zhang, Wenkai Zhu, Chi Zhang, Joseph Peoples, Xuan Li, Andrea Lorena Felicelli, Xiwei Shan, David M. Warsinger, Theodorian Borca-Tasciuc, Xiulin Ruan,* and Tian Li*

Read Online

ACCESS | 📊 Metrics & More | 📖 Article Recommendations | 🆂🅸 Supporting Information

ABSTRACT: Atmospheric water harvesting (AWH) has received tremendous interest because of population growth, limited freshwater resources, and water pollution. However, key challenges remain in developing efficient, flexible, and lightweight AWH materials with scalability. Here, we demonstrated a radiative cooling fabric for AWH via its hierarchically structured cellulose network and hybrid sorption−dewing mechanisms. With 8.3% solar absorption and ~0.9 infrared (IR) emissivity, the material can drop up to 7.5 °C below ambient temperature without energy consumption via radiative cooling. Water adsorption onto the hydrophilic functional groups of cellulose is dominated by sorption at low relative humidity (RH) and dewing at high RH. The cellulose network provides desirable mechanical properties with entangled high-aspect-ratio fibers over tens of adsorption−extraction cycles. In the field test, the cellulose sample exhibited water uptake of 1.29 kg/kg at 80% RH during the night. The profusion of radiative cooling fabric features desirable cost effectiveness and allows fast deployment into large-scale AWH applications.

KEYWORDS: cellulose, radiative cooling, atmospheric water harvesting, energy efficiency, sustainability, large scale
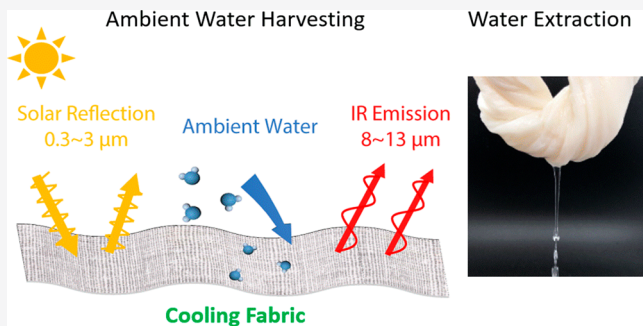

INTRODUCTION

Atmospheric water is ubiquitous regardless of geological or hydrological conditions. Extracting water from the air is a promising method of providing families and communities with off-grid access to safe drinking water, especially for developing countries.[1−4] Significant developments have been achieved by physical dewing[5−12] or chemical sorption[13−28] as the two major collection mechanisms. The typical materials for physical dewing include poly(methyl methacrylate),[5] poly-tetrafluoroethylene,[11] polyethylene foil,[6,7,12] hydrophilic foil,[10] and a durable enhanced specular reflector metal.[9] Sorption-based AWH materials utilize the chemical adsorption and desorption cycles that work across a wide range of relative humidity (RH) (20−100%) via substances' chemical hydro-philicity (e.g., metal−organic framework, salts)[13,15−21,28−30] or the molecular structures that encapsulate water vapor between molecular chains (e.g., zeolites, silica gels, and super-moisture-absorbent gels).[14,22−25,27,31] Given all of these promising advances, challenges remain in (1) improving the energy efficiency when operating at low RH where the dew point and ambient temperature differ greatly, (2) developing more energy-efficient and low-carbon-footprint materials that do not involve complex material synthesis and costly chemicals, and (3) scalable deployment that is not limited by the technologies and material availability.

Cellulose, which comprises ~90% cotton and ~50% wood, is the most abundant organic polymer on earth, featuring good mechanical strength, strong water retention, low cost, and low weight.[32−34] In this work, we used a cellulose-based fabric as a functional radiative cooling scaffold to enable cost-effective ambient water harvesting. Figure 1 illustrates the hierarchical porous structure of the material and the multiscale sorption mechanisms. The highly porous fiber network of cellulose fabric acts as an optical scattering center, reflecting 47% of the incoming irradiation in the solar spectrum. The low solar absorption that originates from the low optical loss of the cellulose fibers and the material's disordered microstructure prevents the temperature rise of the material. The numerous naturally occurring micro- and nanostructured fibers in cellulose-based fabrics strongly emit in the infrared range through the atmospheric transparent window (8−13 μm) to outer space via molecular vibrations, which result in effective cooling of the sample via radiation heat transfer. The achieved lower temperature facilitates exothermic water harvesting.
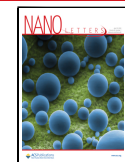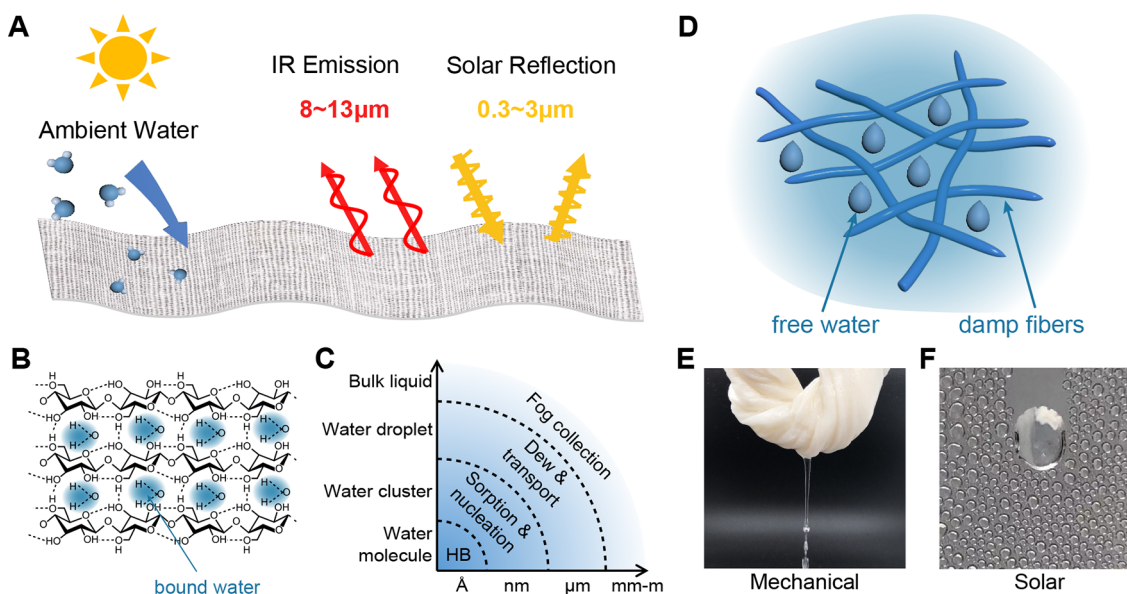
**Figure 1.** Energy-efficient atmospheric water adsorption and extraction with radiative cooling cellulose. (A) Schematic of atmospheric water harvesting by radiative cooling fabric. (B) Molecular cellulosic chains for efficient water molecule adsorption. (C) Multiscale cellulose−water interactions from molecular (Å), nanoporous (nm), microporous (μm), and macroscopic (mm-m) scales. HB refers to hydrogen bonding. (D) Cooled cellulose scaffolds with physically entangled fibers and trapped water. Photograph of water extraction by (E) mechanical squeezing and (F) solar heating.
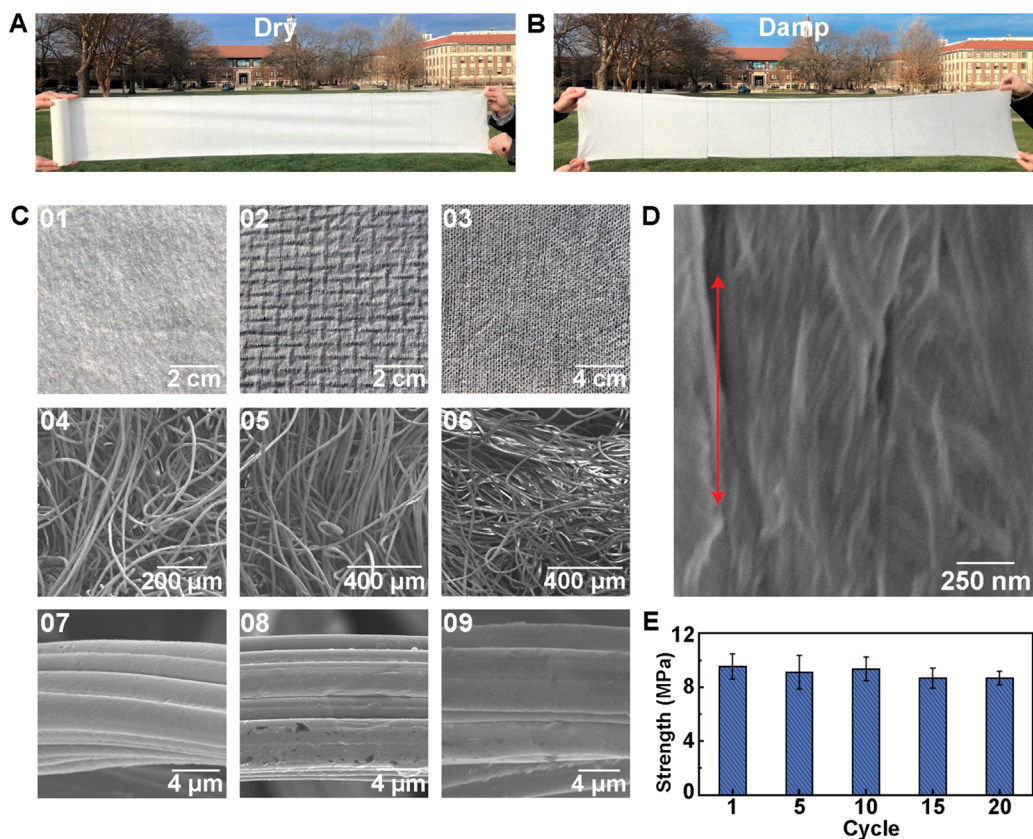
Figure 2. Macro-/microstructures and mechanical properties of cellulose fabric. Photographs of large-scale cellulose fabric under (A) dry and (B) damp conditions with a width of 25 cm. (C) (01−03) Photographs and (04−06) SEMs of different fabric samples composed of entangled cellulose fiber bundles and (07−09) magnified views of fibers within bundles. The images in the same column are from the same sample. (D) SEM image of partially aligned nanofibers. The arrow indicates the nanofiber alignment direction. (E) Mechanical strength over 1, 5, 10, 15, and 20 adsorption−extraction cycles of the fabric sample.

Figure 1B shows that hydroxyl groups of cellulose chains strongly attract water via hydrogen bonding. The innate hydrophilicity of the cellulose fibers enhances the water adsorption by reducing the nucleation energy barrier of
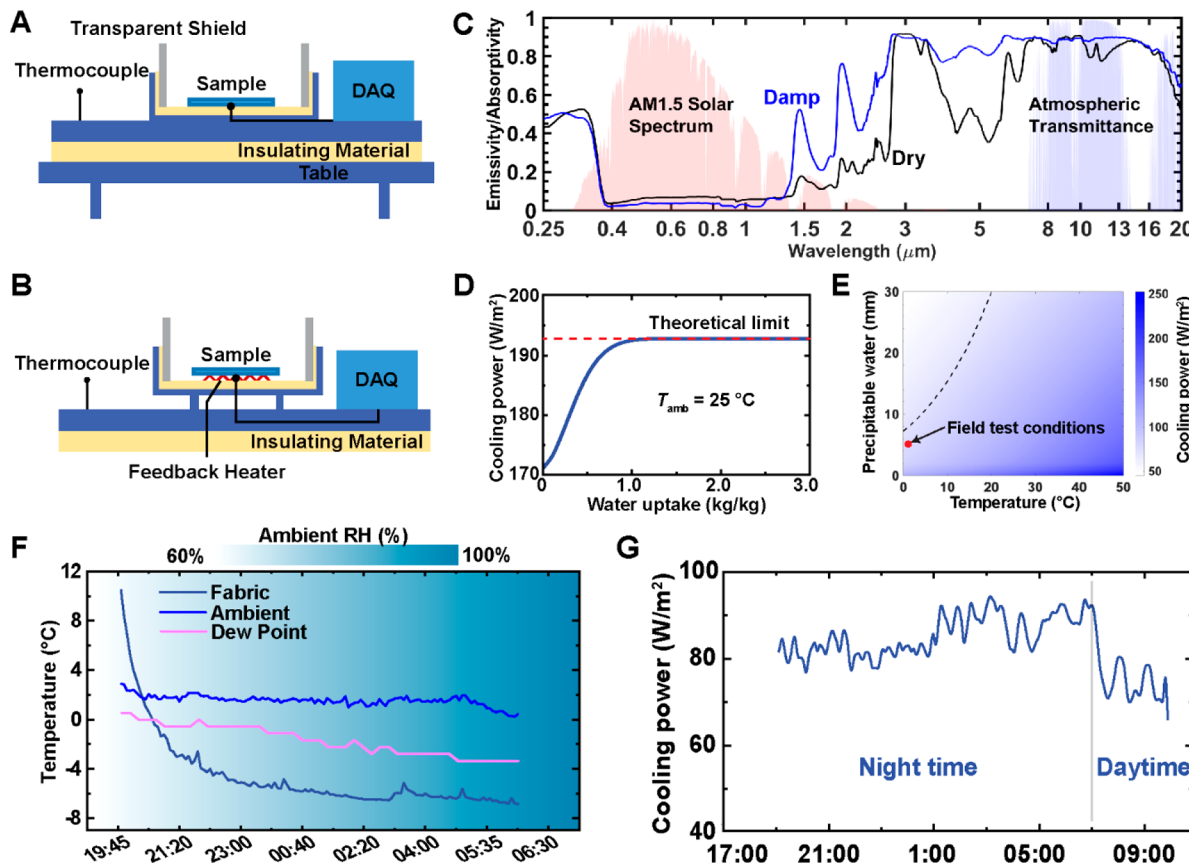
Figure 3. Optical and thermal characterization of the cellulose-based fabric with field validation. (A) Schematic of the temperature measurement setup. (B) Cooling power experimental setup. The sample was maintained at the same temperature as the ambient by a feedback heater. The power output of the feedback heater is regarded as the cooling power. (C) Emissivity in the ultraviolet, visible, and infrared range of the fabric under dry and damp conditions. (D) Theoretical cooling power as a function of water uptake of the fabric sample. (E) Theoretical cooling power as a function of precipitable water and ambient temperature. The dashed line traces PW of 100% RH at different ambient temperatures. (F) Profiles of the sample surface temperatures and ambient temperature on Nov 11, 2020. The RH is represented by the colored background. The sample's temperature dropped rapidly at the beginning of the field test because of the high initial temperature. (G) Profile of the cooling power measured between 19:00 and 9:30 on Jan 20, 2021. The ambient conditions of the field test are also indicated in panel E.

condensation,[35] and the bonded water molecules also attract more water vapor.[36] The cross-linked cellulosic polymer chains provide cages for retaining the adsorbed water.[37] Dew condensation occurs when the cellulose surface temperature is lower than the dew point and the free water is formed mostly in the microscale fibril network (Figure 1C). The physical entanglement and morphology of the large-aspect-ratio fiber bundles (Figure 1D) impart strong mechanical strength and water-trapping abilities. Thus, our material can be rolled or folded to extract the adsorbed water by mechanical compression or heating (Figure 1E,F). Both heating and mechanical loading raise the chemical potential of the adsorbed water, thus pushing the equilibrium toward desorption. Because of the biocompatibility of cellulose, extracted water does not present toxic elements or excess ions. Impurities from ambient water can be filtered during extraction by the multiscale pores of the cellulose. Furthermore, the high durability is evident by the stable performance after many adsorption−extraction cycles. A low carbon footprint and environmental impact are expected because of the minimized requirements in synthesis and recyclability. Thus, the inherent material and structural advantages of cellulose enable energy-efficient, cost-effective, lightweight, and distributable AWH systems that can provide drinking water for individuals and communities.

■ STRUCTURAL ANALYSIS

Cellulose-based fabrics are easily scalable (Figure 2A,B) and abundant in daily use. The samples feature a hierarchical structure as revealed by the optical microscope images (Figures S1 and S2) and scanning electron microscope (SEM) images. An aspect ratio greater than 100 and a fiber length greater than 1.5 mm are observed (Figure 2C04−06). The long fibers and partially densified fiber network provide strong physical entanglement, leading to desirable flexibility and high mechanical strength (Note S2). The microscale cellulose fibers (Figure 2C07−09) are further composed of aligned cellulose nanofibers (Figure 2D). An overall porosity of >90% is estimated for all tested fabrics where the exemplified fabric sample has 95.1% porosity (Note S3). Figure 2E presents the tensile strength variation of the fabric after 20 adsorption−extraction cycles. Throughout 20 cycles, the mechanical strength exhibits a negligible change for both samples with a strength of ∼9 MPa. The variation of the mechanical strength of the fabric samples is mainly attributed to (1) the nonuniformity of structural morphology, such as the random arrangement of the fibers, and (2) the difference in fiber aspect ratios.[32] The nondegrading mechanical strength reveals the robustness and durability of the cellulose fabric and supports
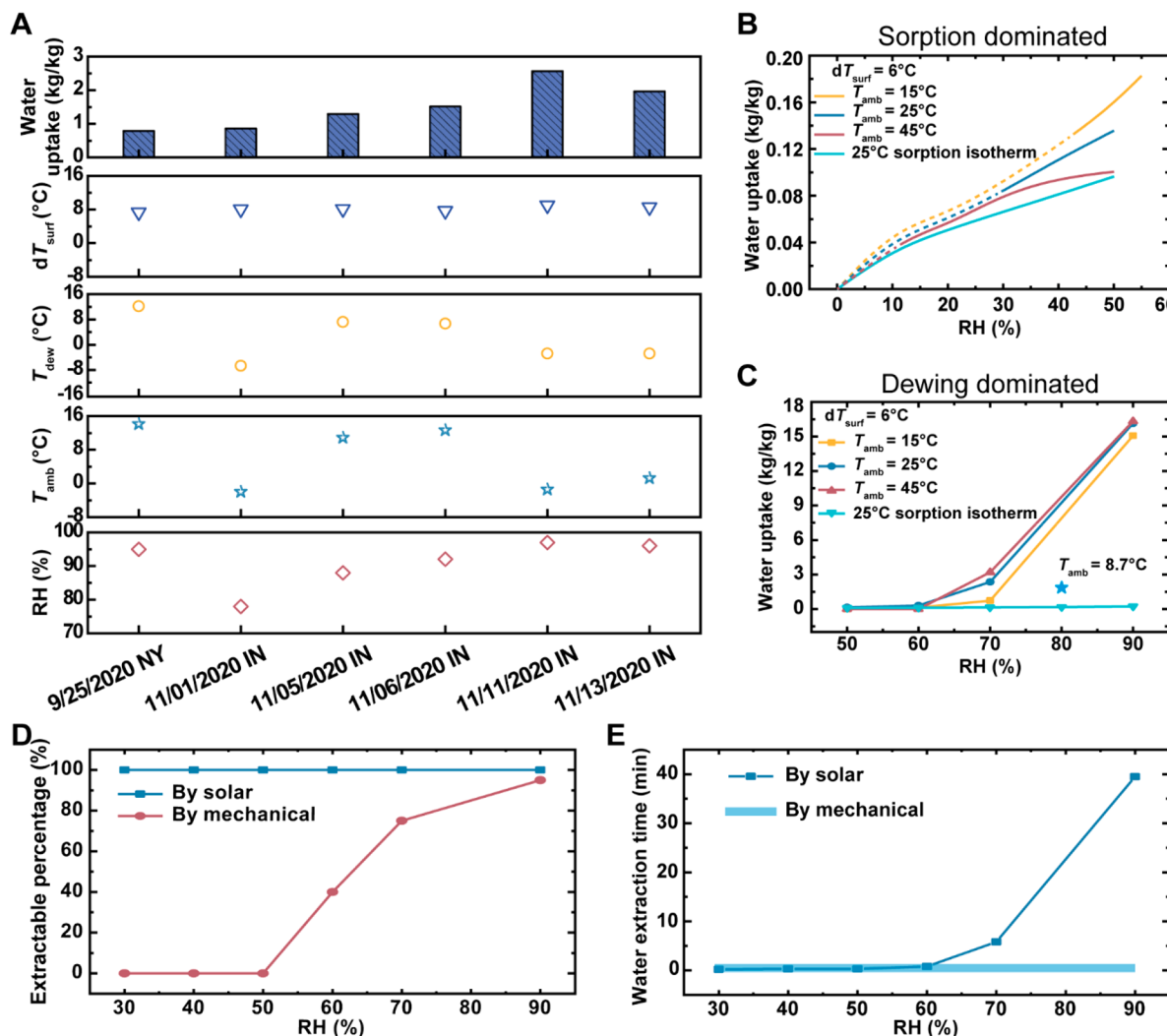
Figure 4. Quantity of water collection by cellulose fabric in the field test under laboratory conditions. (A) Summaries of AWH performance of the cellulose sample and ambient conditions for the five representative field tests in Troy, NY and West Lafayette, IN. (B) Water uptake for cellulose sample of 6 °C temperature below ambient at ambient temperatures 15, 25, 45 °C and RH of 12−50% where sorption dominates the water uptake. The dashed line is an extrapolation curve based on the measured data. The sorption isotherm at 25 °C is plotted as a reference line. (C) Water uptake for a cellulose sample exhibiting a 6 °C temperature drop below ambient at ambient temperatures of 15, 25, and 45 °C and an RH of 50−90% where condensation dominates the water uptake. The sorption isotherm at 25 °C is plotted as a reference line, and the star denotes the water uptake under conditions similar to those of the Nov 5 field test. (D) Extractable water percentage by solar power and mechanical compression of 30−90% RH. (E) Water extraction time by solar power and mechanical compression for a sample at 30−90% RH.

the viability of employing a mechanical water extraction method over an extended lifetime.

RESULTS AND DISCUSSION

The cellulose-based fabric is investigated in the field test setups at night, as demonstrated in Figure 3A,B. The investigation of the solar absorption and the atmospheric transparent window (8−13 μm) emissivity of the cellulose fabric sample in the wavelength range between 250 nm and 20 μm is shown in Figure 3C and Note S4. The cellulose fabric samples have a low optical absorption of incident sunlight due to the microscale pores and the coarser surfaces of fibers (Figure 2E07−09). At the same time, the multimode molecular vibrations, including the O−H stretching vibration and C−O−H bending,[38] facilitate strong emission in the infrared (IR) region. Thermal radiation from the cellulose fabric, particularly at wavelengths in the atmospheric transparency window, can penetrate the atmosphere and utilize deep space (with a

uniform blackbody temperature of 2.73 K[39]) as the heat sink, resulting in a highly efficient and isotropic radiative cooling effect. The cooling effect will significantly lower the sample temperature. Interestingly, the effective emissivity over the atmospheric transparency window is 0.86 for the fabric sample in a dry environment and is enhanced to 0.89 when it is damp. The emissivity improvement of 0.03 in a damp environment is mainly attributed to the adsorbed water in the micropores where (1) the additional bonding between the OH⁻ branches and H$_2$O molecules complement the missing molecular vibrational modes and (2) the high emissivity of water in the IR spectrum significantly contributes to higher thermal emission.[40] Consequently, the water adsorption process will enhance the cooling of cellulose samples, which in turn benefits water harvesting. An analytical model of the cellulose thermodynamic system is used to quantitatively evaluate the theoretical nighttime cooling power at different water uptake based on the rule of mixtures (Note S5). It is shown that the

higher cooling power is associated with increased water uptake because the accumulated water can potentially boost the nighttime cooling power of the fabric toward the theoretical limit of 192.8 W/m^2 (calculated with unity emissivity from 2 to 20 μm and the atmospheric transmittance spectrum at zero precipitable water) (Figure 3D). Because high relative humidity occurs during harvesting, its impact on the sample's theoretical cooling power is also evaluated. Precipitable water (PW) is used to indicate the RH level (100% RH corresponds to ~40 mm at 25 °C and 1 atm) and as a variable that affects the transmissivity and emissivity spectrum of the atmosphere. A higher amount of precipitable water increases the radiative power from the atmosphere (eq 1) and negatively impacts the cooling performance

$$P_{atm}(T_{atm}, PW) = \int_0^{\pi/2} \int_0^{\infty} 2\pi \, \sin(\theta) \, \cos(\theta) \, \varepsilon_s(\lambda, \theta)$$
$$\varepsilon_{atm}(\lambda, \theta, PW) \, I_{BB}(T_{atm}, \lambda) \, d\lambda \, d\theta \quad (1)$$

where P, T, θ, ε, λ, and I_{BB} are the power density, temperature, azimuthal angle, emissivity, wavelength, and blackbody radiation determined from Planck's law, respectively. Subscripts s and atm refer to the sample and atmosphere, respectively. Figure 3E maps the theoretical cooling power from 0 to 50 °C ambient temperature and 0 to 30 mm precipitable water. This model does not include the synergetic effect due to the higher emissivity of the adsorbed water under high humidity, making it a conservative estimate of the cooling power.[41] The dashed line of 100% RH and the minimum 50 W/m^2 cooling power justify that radiative cooling is still viable under high relative humidity to aid water harvesting.

The schematics of the field-test apparatus utilized to experimentally demonstrate the radiative cooling surface temperature and cooling power of cellulose samples are illustrated in Figure 3A,B. The field tests of subambient radiative cooling were conducted during September in Troy, NY (42.7284° N, 73.6918° W) and were repeated between November and January in West Lafayette, IN (40.4237° N, 86.9212° W) from ~ 9:00 pm to 6:30 am. During each field test, the cellulose surface temperature, ambient temperature, and dew-point temperature were monitored simultaneously (Figure 3A, Note S6). Figure 3F highlights the maximum surface temperature drop of 8.1 °C for the fabric sample at ~90% RH during one night (Nov 11). Throughout the field tests (Sept 25−Dec 9, 2020), the temperature profiles of the sample exhibit continuous and consistent subambient cooling, with an average of 7.5 °C below ambient temperature (dT_{surf}) observed during the night, where dT_{surf} is defined as the sample temperature minus ambient temperature (T_{amb}). An average radiative cooling power of 82.7 W/m^2 was measured with a feedback heater (Figure 3B, Note S7) for the fabric during the nights of Jan 19−21, 2021 (Figure 3G), which is consistent with the theoretical model. Note that the cooling power and the temperature drop below ambient values of the sample surface vary with ambient conditions (i.e., temperature, RH, and cloud conditions).

To fully understand the effect of ambient conditions (i.e., RH and T_{amb}) on cellulose-based AWH, the sample is tested in an environmental chamber (Note S8) with controlled T_{amb} (15, 25, 45 °C) and RH (12−90%). The conditions were selected on the basis of global climate variations and are also similar to the test conditions of others.[14,15] By analogy to the cooling effect in an environmental chamber, the sample

temperature is held constant by a thermoelectric device at 6 °C below the ambient temperature (Figure S9), which is the typical average temperature drop during the field test (Figure 4A). We evaluate the heat release by the phase change as compared to the radiative cooling power, considering the inherently high heat capacity and phase change enthalpy (latent heat = 2440 kJ/kg = 677 kWh/m^3 at 25 °C)[42] associated with dew condensation. With the field test water uptake (2.38 kg/kg), cooling power (60−80 W/m^2), duration (8 h), and low area density of the sample (0.0416 kg/m^2), the estimated condensation heat release occupies only 10.5−14.0% of the net radiative cooling energy by eq 2 (Note S9). Clearly, although a small fraction of the cooling power is offset by the heat release of condensation, the condensed water will fill the macropores and the water will contribute to the radiative cooling by its high IR emissivity. Therefore, quasi-steady-state equilibrium can be achieved with little variation in ambient conditions on the minute time scale and a constant temperature drop below ambient that can be assumed at different relative humidities for a laboratory test

$$Q_{cooling} = Q_{phase\,change} + Q_{steady\,state} \quad (2)$$

where Q being the energy density with units of kJ/m^2.

Water uptake increases with operating time until the amount of water in cellulose samples is saturated (Figure S10). The water uptake profiles (Figure S10B) at 6 °C below the ambient temperature indicate that the cellulose fabric takes 1−3 h to achieve a steady-state water uptake at 25 °C ambient temperature. Figure 4B,C depicts the saturated water uptake as a function of RH. The sorption process mainly forms bounded water at low RH, and dew condensation occurs when the RH is >60% with a surface temperature that is 6 °C lower than the ambient temperature. In general, sorption and condensation analyses show that radiative cooling has a positive impact on both phenomena. Although the water sorption at the lower end of the spectrum is inferior to that of other reported AWH systems[21,43,44] (Table S2), the advantages of potential zero energy input and scalability are unique to the radiative cooling AWH system by the hybrid sorption-dewing fabric. A 6 °C temperature drop of the cellulose fabric increases water uptake by 1.3 times at 30% RH (sorption-dominated) and by 70 times at 90% RH (condensation-dominated) compared to the sample's sorption isotherm (Note S10). The concept of lowering the temperature by a radiative cooling effect can inspire other AWH materials or systems.

Because of local vapor saturation and the cooling-induced phase change, more water adsorption is observed during dew condensation than the sorption process. The porous structure provides a low area density and leads to a high water uptake as defined per unit mass. With the foldable feature, the low area density highlights the low weight and portability of this material. During water adsorption, the passively cooled fiber network lowers the water activity under a 25 °C ambient condition, shifts up the sorption isotherm, and reduces the fiber temperature (Figure 4B). The cooled sample can even reach a temperature below the dew point toward local condensation when the RH is >60% (Figure 4C). Conversely, the fiber−water interaction and the water adsorbed on the fibers will increase the overall IR emissivity of the sample compared to that of fibers alone, leading to a higher cooling power. Under conditions (8.7 °C ambient temperature) close to those of the Nov 5 field test, the cellulose sample 6 °C
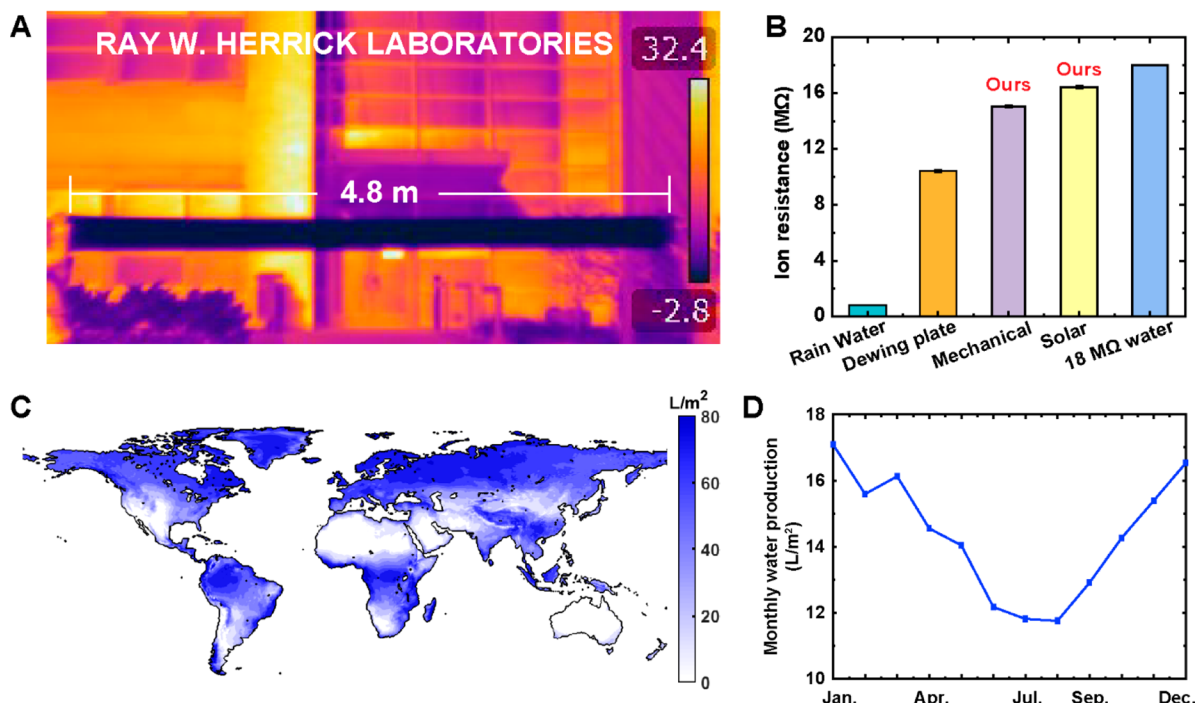
Figure 5. Scalability, impact, and the prospect of AWH by radiative cooling cellulose material. (A) IR image of a large-scale cellulose sample taken in front of the Ray. W. Herrick Laboratories, Purdue University at 1 °C ambient temperature and 50% RH. The sample has a very low temperature compared to the ambient temperature. (B) Ion conductivity test of water for different collection processes. (C) Cumulative annual water collection solely by cellulose-based AWH, with the prediction based on the local climate around the globe. (D) Spatially averaged monthly water production per area.

below the ambient temperature at 80% RH yields a similar water uptake of 1.89 kg/kg (i.e., 0.079 L/m²) (Figure 4C, star data point). Ambient air at 25 °C and 90% RH in the laboratory test has a saturated vapor pressure that is 3.2 times higher than that of air at 8.7 °C and 80% RH in the field test. The difference between the absolute amount of water and other unpredictable environmental fluctuations leads to the overall higher water uptake in the laboratory test than in the field test. In the water extraction process, the sample can be either mechanically squeezed or heated by solar power depending on the availability of the energy sources (Note S11). The time consumption and extractable water percentage of solar heating and mechanical compression are shown in Figure 4D,E. Solar heating can extract 100% of the adsorbed water at 30−90% RH. Using a 500 N load (typical hand grip strength),[45] the water can be extracted by mechanical compression when the RH is >60%. The curve of extraction time vs RH by solar heating follows a trend similar to water uptake vs RH because an increasing sample area simultaneously promotes the adsorbed water and absorbed solar energy. In contrast, the extraction time of mechanical compression is negligible.

■ LARGE-SCALE IMPACT

The cellulose-based AWH also features high portability and scalability for large-scale deployment. Effective radiative cooling under direct solar irradiation is observed, as evidenced by the IR images of the large-scale cellulose samples (Figure 5A). Water quality is another crucial aspect of the design and development of AWH. To test the effect of cellulose for water purification, the electrical resistance of collected water in the outdoor experiments is measured to indicate ion conductivity

(a higher ion resistance indicates high purity of the water[46]). During water extraction, our porous cellulose fabric can potentially filter water via the electrostatic interaction between the surface-charged fiber network and impurities.[47] Figure 5B presents the resistances of collected water and the standard 18 MΩ purified water. In comparison, rainwater exhibits the lowest ionic resistance (0.02 MΩ), indicating the highest concentration of impurities. This is likely due to the fact that precipitation droplets are formed by nucleating around floating particles such as dirt and dust. Water originating from mechanical and solar extraction gives ionic resistances of 15.03 and 16.43 MΩ, respectively. Compared to the water condensed directly on the dewing plate, our radiative cooling cellulose material harvests water with 50.8 and 64.8% higher resistances by mechanical extraction and by solar extraction, respectively, as a result of the filtration effect of the fiber network. The comparable resistances to the highly purified standard 18 MΩ water indicate the cellulose material's capability of generating safe and clean water regardless of the ambient air quality. Furthermore, to avoid dust and particles clogging, the fabric sample can be washed and disinfected via bleaching after cyclic use.

Potential daily water production on a global scale is estimated using the performance characterized in the laboratory test (Figure 4B,C). The model uses the global climate data from the National Centers for Environmental Prediction (NCEP) for the year 2020[48] and interpolates the amount of daily water production based solely on the local relative humidity. The conservative estimation assumes that water production occurs only one-third of a year (functional days) and for only one adsorption−extraction cycle every functional day that excludes unfavorable climate conditions (Note S12). The annual production of a minimum of 2 L/m²

and a maximum of 80 L/m^2 establishes a baseline pattern for the continents (Figure 5C). The cellulose fabric is predicted to have a greater monthly water production between October and March (Figure 5D). Furthermore, with an extremely low raw material cost, the annual cost of water production was estimated to be as low as $5.2/L at 60% RH and $0.01/L at 90% RH. Together with its durability and sustainability, the large-scale potential of cellulose-based fabric can translate to a fast and distributed deployment for household use as a value-added cellulose product, opening abundant but largely unexplored industrialization opportunities with the new fundamental properties of cellulose revealed.

■ CONCLUSIONS

In this work, we report scalable, efficient, and sustainable atmospheric water harvesting with a passive radiative cooling cellulose-based fiber network. The excellent passive radiative cooling capability of cellulose provides an average sample temperature that is up to 7.5 °C lower than the ambient temperature for enhanced nighttime water uptake. In addition, the naturally occurring hierarchical structure of the hydrophilic cellulose fiber network enables a multiscale, synergistic interaction of cellulose, water, and energy. A high harvesting capacity was demonstrated under both controlled and natural conditions. By estimation, an average annual water production of 40 L/m^2, solely by AWH, can be potentially realized by simply spreading out cellulose-based fabric toward the sky during the night. The portability of cellulose fabric further extends the scope of AWH. With the understanding of the merit of combining sorption and radiative cooling, further material optimization can target an improved optical response, mechanical properties, and hygroscopicity. A further enhancement of the IR emissivity and reduction of the solar reflectivity are desired for future improvement. The fiber network can be redesigned for fewer macroscopic holes and more closely packed fibers for higher mechanical robustness and cyclability. Potential hygroscopic functional groups can be incorporated into the cellulose or engineered as cellulose derivatives for greater water harvesting. Our approach to utilizing natural materials and energy-efficient water-harvesting mechanisms such as radiative cooling and mechanical squeezing can potentially enable new opportunities in effectively harvesting ambient water in a sustainable, cost-effective, and scalable way.

■ ASSOCIATED CONTENT

Ⓢ Supporting Information

The Supporting Information is available free of charge at https://pubs.acs.org/doi/10.1021/acs.nanolett.1c04143.

> Materials and Methods and supplementary figures and tables (PDF)

■ AUTHOR INFORMATION

Corresponding Authors

Xiulin Ruan − *School of Mechanical Engineering, Purdue University, West Lafayette, Indiana 47907, United States;* ⓞ orcid.org/0000-0001-7611-7449; Email: ruan@purdue.edu

Tian Li − *School of Mechanical Engineering, Purdue University, West Lafayette, Indiana 47907, United States;* ⓞ orcid.org/0000-0002-1087-0662; Email: tianli@purdue.edu

Authors

Yun Zhang − *School of Mechanical Engineering, Purdue University, West Lafayette, Indiana 47907, United States*

Wenkai Zhu − *School of Mechanical Engineering, Purdue University, West Lafayette, Indiana 47907, United States*

Chi Zhang − *Department of Mechanical and Process Engineering, ETH Zurich, 8092 Zurich, Switzerland;* ⓞ orcid.org/0000-0002-9018-0492

Joseph Peoples − *School of Mechanical Engineering, Purdue University, West Lafayette, Indiana 47907, United States;* ⓞ orcid.org/0000-0002-0495-1394

Xuan Li − *School of Mechanical Engineering, Purdue University, West Lafayette, Indiana 47907, United States*

Andrea Lorena Felicelli − *School of Mechanical Engineering, Purdue University, West Lafayette, Indiana 47907, United States*

Xiwei Shan − *School of Mechanical Engineering, Purdue University, West Lafayette, Indiana 47907, United States*

David M. Warsinger − *School of Mechanical Engineering, Purdue University, West Lafayette, Indiana 47907, United States; Birck Nanotechnology Center, Purdue University, West Lafayette, Indiana 47907, United States*

Theodorian Borca-Tasciuc − *Mechanical, Aerospace, and Nuclear Engineering Department, Rensselaer Polytechnic Institute, Troy, New York 12180, United States*

Complete contact information is available at:
https://pubs.acs.org/10.1021/acs.nanolett.1c04143

Author Contributions

.L., X.R., T.B., and D.W. designed the experiments. Y.Z., W.Z., C.Z. carried out the analysis. Y.Z., W. Zhu, J.P., X.L., A.F., and X.S. conducted the experiments and contributed to data illustration. All co-authors contributed to manuscript writing.

Notes

The authors declare no competing financial interest.

■ ACKNOWLEDGMENTS

■ REFERENCES

(1) Klemm, O.; Schemenauer, R. S.; Lummerich, A.; Cereceda, P.; Marzol, V.; Corell, D.; Van Heerden, J.; Reinhard, D.; Gherezghiher, T.; Olivier, J. Fog as a Fresh-Water Resource: Overview and Perspectives. *Ambio* **2012**, *41* (3), 221−234.

(2) Khalil, B.; Adamowski, J.; Shabbir, A.; Jang, C.; Rojas, M.; Reilly, K.; Ozga-Zielinski, B. A Review: Dew Water Collection from Radiative Passive Collectors to Recent Developments of Active Collectors. *Sust. Wat. Resour. Man.* **2016**, *2* (1), 71−86.

(3) Mekonnen, M. M.; Hoekstra, A. Y. Four Billion People Facing Severe Water Scarcity. *Sci. adv.* **2016**, *2* (2), 1500323.

(4) Li, Z.; Xu, X.; Sheng, X.; Lin, P.; Tang, J.; Pan, L.; Kaneti, Y. V.; Yang, T.; Yamauchi, Y. Solar-Powered Sustainable Water Production: State-of-the-Art Technologies for Sunlight-Energy-Water Nexus. *ACS Nano* **2021**, *15* (8), 12535−12566.

(5) Beysens, D.; Muselli, M.; Milimouk, I.; Ohayon, C.; Berkowicz, S. M.; Soyeux, E.; Mileta, M.; Ortega, P. Application of Passive

Radiative Cooling for Dew Condensation. *Energy* **2006**, *31* (13), 2303−2315.

(6) Muselli, M.; Beysens, D.; Marcillat, J.; Milimouk, I.; Nilsson, T.; Louche, A. Dew Water Collector for Potable Water in Ajaccio (Corsica Island, France). *Atmos. Res.* **2002**, *64* (1−4), 297−312.

(7) Muselli, M.; Beysens, D.; Milimouk, I. A Comparative Study of Two Large Radiative Dew Water Condensers. *J. Arid Environ.* **2006**, *64* (1), 54−76.

(8) Liu, C.; Wu, Y.; Wang, B.; Zhao, C. Y.; Bao, H. Effect of Atmospheric Water Vapor on Radiative Cooling Performance of Different Surfaces. *Sol. Energy* **2019**, *183*, 218−225.

(9) Liu, C.; Fan, J.; Bao, H. Hydrophilic Radiative Cooler for Direct Water Condensation in Humid Weather. *Sol. Energy Mater. Sol. C* **2020**, *216*, 110700.

(10) Maestre-Valero, J.; Martinez-Alvarez, V.; Baille, A.; Martín-Górriz, B.; Gallego-Elvira, B. Comparative Analysis of Two Polyethylene Foil Materials for Dew Harvesting in a Semi-Arid Climate. *J. hydrol.* **2011**, *410* (1−2), 84−91.

(11) Clus, O.; Ortega, P.; Muselli, M.; Milimouk, I.; Beysens, D. Study of Dew Water Collection in Humid Tropical Islands. *J. Hydrol.* **2008**, *361* (1−2), 159−171.

(12) Maestre-Valero, J.; Martin-Gorriz, B.; Martínez-Alvarez, V. Dew Condensation on Different Natural and Artificial Passive Surfaces in a Semiarid Climate. *J. Arid Environ.* **2015**, *116*, 63−70.

(13) Fathieh, F.; Kalmutzki, M. J.; Kapustin, E. A.; Waller, P. J.; Yang, J.; Yaghi, O. M. Practical Water Production from Desert Air. *Sci. adv.* **2018**, *4* (6), 3198.

(14) Zhao, F.; Zhou, X.; Liu, Y.; Shi, Y.; Dai, Y.; Yu, G. Super Moisture-Absorbent Gels for All-Weather Atmospheric Water Harvesting. *Adv. Mater.* **2019**, *31* (10), 1806446.

(15) Kim, H.; Yang, S.; Rao, S. R.; Narayanan, S.; Kapustin, E. A.; Furukawa, H.; Umans, A. S.; Yaghi, O. M.; Wang, E. N. Water Harvesting from Air with Metal-Organic Frameworks Powered by Natural Sunlight. *Science* **2017**, *356* (6336), 430−434.

(16) Gong, F.; Li, H.; Zhou, Q.; Wang, M.; Wang, W.; Lv, Y.; Xiao, R.; Papavassiliou, D. V. Agricultural Waste-Derived Moisture-Absorber for All-Weather Atmospheric Water Collection and Electricity Generation. *Nano Energy* **2020**, *74*, 104922.

(17) Li, R.; Shi, Y.; Wu, M.; Hong, S.; Wang, P. Improving Atmospheric Water Production Yield: Enabling Multiple Water Harvesting Cycles with Nano Sorbent. *Nano Energy* **2020**, *67*, 104255.

(18) Yao, H.; Zhang, P.; Huang, Y.; Cheng, H.; Li, C.; Qu, L. Highly Efficient Cean Water Production from Contaminated Air with a Wide Humidity Range. *Adv. Mater.* **2020**, *32* (6), 1905875.

(19) Canivet, J.; Bonnefoy, J.; Daniel, C.; Legrand, A.; Coasne, B.; Farrusseng, D. Structure-Property Relationships of Water Adsorption in Metal-Organic Frameworks. *New J. Chem.* **2014**, *38* (7), 3102−3111.

(20) Cadiau, A.; Lee, J. S.; Damasceno Borges, D.; Fabry, P.; Devic, T.; Wharmby, M. T.; Martineau, C.; Foucher, D.; Taulelle, F.; Jun, C. H. Design of Hydrophilic Metal Organic Framework Water Adsorbents for Heat Reallocation. *Adv. Mater.* **2015**, *27* (32), 4775−4780.

(21) Kim, H.; Rao, S. R.; Kapustin, E. A.; Zhao, L.; Yang, S.; Yaghi, O. M.; Wang, E. N. Adsorption-Based Atmospheric Water Harvesting Device for Arid Climates. *Nat. commun.* **2018**, *9* (1), 1−8.

(22) Alam, M. N.; Christopher, L. P. Natural Cellulose-Chitosan Cross-Linked Superabsorbent Hydrogels with Superior Swelling Properties. *ACS Sustain. Chem. Eng.* **2018**, *6* (7), 8736−8742.

(23) Matsumoto, K.; Sakikawa, N.; Miyata, T. Thermo-Responsive Gels that Absorb Moisture and Ooze Water. *Nat. commun.* **2018**, *9* (1), 1−7.

(24) Xu, J.; Li, T.; Yan, T.; Wu, S.; Wu, M.; Chao, J.; Huo, X.; Wang, P.; Wang, R. Ultrahigh Solar-Driven Atmospheric Water Production Enabled by Scalable Rapid-Cycling Water Harvester with Vertically Aligned Nanocomposite Sorbent. *Energy Environ. Sci.* **2021**, *14* (11), 5979−5994.

(25) Nandakumar, D. K.; Ravi, S. K.; Zhang, Y.; Guo, N.; Zhang, C.; Tan, S. C. A Super Hygroscopic Hydrogel for Harnessing Ambient Humidity for Energy Conservation and Harvesting. *Energy Environ. Sci.* **2018**, *11* (8), 2179−2187.

(26) Ejeian, M.; Wang, R. Adsorption-Based Atmospheric Water Harvesting. *Joule* **2021**, *5* (7), 1678−1703.

(27) Zhou, X.; Zhang, P.; Zhao, F.; Yu, G. Super Moisture Absorbent Gels for Sustainable Agriculture via Atmospheric Water Irrigation. *ACS Mater. Lett.* **2020**, *2* (11), 1419−1422.

(28) Nguyen, H. L.; Hanikel, N.; Lyle, S. J.; Zhu, C.; Proserpio, D. M.; Yaghi, O. M. A Porous Covalent Organic Framework with Voided Square Grid Topology for Atmospheric Water Harvesting. *J. Am. Chem. Soc.* **2020**, *142* (5), 2218−2221.

(29) Deng, F.; Wang, C.; Xiang, C.; Wang, R. Bioinspired Topological Design of Super Hygroscopic Complex for Cost-Effective Atmospheric Water Harvesting. *Nano Energy* **2021**, *90*, 106642.

(30) Gordeeva, L. G.; Tu, Y.; Pan, Q.; Palash, M.; Saha, B. B.; Aristov, Y. I.; Wang, R. Metal-Organic Frameworks for Energy Conversion and Water Harvesting: A Bridge between Thermal Engineering and Material Science. *Nano Energy* **2021**, *84*, 105946.

(31) Hua, L.; Xu, J.; Wang, R. Exergy-Efficient Boundary and Design Guidelines for Atmospheric Water Harvesters with Nano-Porous Sorbents. *Nano Energy* **2021**, *85*, 105977.

(32) Li, T.; Chen, C.; Brozena, A. H.; Zhu, J. Y.; Xu, L.; Driemeier, C.; Dai, J.; Rojas, O. J.; Isogai, A.; Wågberg, L.; Hu, L. Developing Fibrillated Cellulose as a Sustainable Technological Material. *Nature* **2021**, *590* (7844), 47−56.

(33) Etuk, V. E.; Oboh, I. O.; Etuk, B. R.; Johnson, E. O.; Egemba, K. Nanocellulose: Types, Sythesis and Applications, The European Conference on Sustainability, Energy & the Environment, 2018 Official Conference Proceedings, 2018.

(34) Lamm, M. E.; Li, K.; Qian, J.; Wang, L.; Lavoine, N.; Newman, R.; Gardner, D. J.; Li, T.; Hu, L.; Ragauskas, A. J. Recent Advances in Functional Materials through Cellulose Nanofiber Templating. *Adv. Mater. (Deerfield Beach, Fla.)* **2021**, *33* (12), 2005538.

(35) Seo, D.; Lee, J.; Lee, C.; Nam, Y. The Effects of Surface Wettability on the Fog and Dew Moisture Harvesting Performance on Tubular Surfaces. *Sci. Rep.* **2016**, *6* (1), 1−11.

(36) Zhang, C.; Coasne, B.; Guyer, R.; Derome, D.; Carmeliet, J. Moisture-Induced Crossover in the Thermodynamic and Mechanical Response of Hydrophilic Biopolymer. *Cellulose* **2020**, *27* (1), 89−99.

(37) Kabir, S. F.; Sikdar, P. P.; Haque, B.; Bhuiyan, M. R.; Ali, A.; Islam, M. Cellulose-Based Hydrogel Materials: Chemistry, Properties and Their Prospective Applications. *Prog. biomater.* **2018**, *7* (3), 153−174.

(38) Nguyen, T.-D.; Sierra, E.; Eguiraun, H.; Lizundia, E. Iridescent Cellulose Nanocrystal Films: The Link between Structural Colour and Bragg's Law. *Eur. J. Phys.* **2018**, *39* (4), No. 045803.

(39) Warren, W. S. In *The Physical Basis of Chemistry*, 2nd ed.; Warren, W. S., Ed. Academic Press: San Diego, 2001; Chapter 5, pp 87−127.

(40) Robinson, P.; Davies, J. Laboratory Determinations of Water Surface Emissivity. *J. Appl. Meteorol.* **1972**, *11* (8), 1391−1393.

(41) Peoples, J.; Hung, Y.; Braun, J.; Horton, X. Evaluating the Energy Savings of Radiative Cooling Paints Applied to the Exterior of Buildings. *Int. J. Heat Mass Transfer*, under review, **2022**.

(42) LaPotin, A.; Kim, H.; Rao, S. R.; Wang, E. N. Adsorption-Based Atmospheric Water Harvesting: Impact of Material and Component Properties on System-Level Performance. *Acc. Chem. Res.* **2019**, *52* (6), 1588−1597.

(43) Wang, W.; Xie, S.; Pan, Q.; Dai, Y.; Wang, R.; Ge, T. Air-Cooled Adsorption-Based Device for Hharvesting Water from Island Air. *Renew. Sust. Energy Rev.* **2021**, *141*, 110802.

(44) Tu, Y.; Wang, R.; Zhang, Y.; Wang, J. Progress and Expectation of Atmospheric Water Harvesting. *Joule* **2018**, *2* (8), 1452−1475.

(45) Nilsen, T.; Hermann, M.; Eriksen, C. S.; Dagfinrud, H.; Mowinckel, P.; Kjeken, I. Grip Force and Pinch Grip in an Adult Population: Reference Values and Factors Sssociated with Grip Force. *Scand. J. Occup. ther.* **2012**, *19* (3), 288−296.

(46) Light, T. S.; Licht, S.; Bevilacqua, A. C.; Morash, K. R. The Fundamental Conductivity and Resistivity of Water. *Electrochem. Solid St.* **2005**, *8* (1), E16.

(47) Ottenhall, A.; Henschen, J.; Illergård, J.; Ek, M. Cellulose-Based Water Purification Using Paper Filters Modified with Polyelectrolyte Multilayers to Remove Bacteria from Water through Electrostatic Interactions. *Environ. Sci. Wat. Res.* **2018**, *4* (12), 2070−2079.

(48) Saha, S.; Moorthi, S.; Wu, X.; Wang, J.; Nadiga, S.; Tripp, P.; Behringer, D.; Hou, Y.-T.; Chuang, H.-y.; Iredell, M.; Ek, M.; Meng, J.; Yang, R.; Mendez, M. P.; van den Dool, H.; Zhang, Q.; Wang, W.; Chen, M.; Becker, E. *NCEP Climate Forecast System Version 2 (CFSv2) Selected Hourly Time-Series Products*; Research Data Archive at the National Center for Atmospheric Research; Computational and Information Systems Laboratory: Boulder, CO, 2011. DOI: 10.1175/JCLI-D-12-00823.1.

📖 **Recommended by ACS**

Bioinspired Multilayer Structures for Energy-Free Passive Heating and Thermal Regulation in Cold Environments

Jing Wang, Jin Wang, *et al.*

OCTOBER 07, 2022
ACS APPLIED MATERIALS & INTERFACES

READ ☑

Multifunctional Bamboo Fiber Hybrid Structural Materials for Daytime Radiation Cooling

Xixi Piao, Zhe Wang, *et al.*

NOVEMBER 16, 2022
ACS SUSTAINABLE CHEMISTRY & ENGINEERING

READ ☑

Engineered Wood with Hierarchically Tunable Microchannels toward Efficient Solar Vapor Generation

Tongtong Cui, Chunhong Ye, *et al.*

OCTOBER 14, 2022
LANGMUIR

READ ☑

A Trimode Thermoregulatory Flexible Fibrous Membrane Designed with Hierarchical Core–Sheath Fiber Structure for Wearable Personal Thermal Management

Jiajia Wu, Hideaki Morikawa, *et al.*

AUGUST 10, 2022
ACS NANO

READ ☑

Get More Suggestions >